

CircRNA SMARCC1 Sponges MiR-140-3p to Regulate Cell Progression in Colorectal Cancer

This article was published in the following Dove Press journal:
Cancer Management and Research

Miao-sheng Chen
Cui-hong Lin
Ling-yan Huang
Xiao-ming Qiu

Department of Pathology, Longyan First
Hospital Affiliated to Fujian Medical
University, Longyan, People's Republic of
China

Purpose: Our objective was to investigate the effect of circSMARCC1 on the developmental and biological behavior of colorectal cancer (CRC).

Materials and Methods: The expression of circSMARCC1 and miR-140-3p in CRC tissues and cell lines (SW620, HCT116, HT29 and SW480) and a normal cell line (NCM460) was detected using qRT-PCR. The expression levels of circSMARCC1 and its linear subtype were detected. Fluorescence in situ hybridization was performed for the evaluation of the localization of circSMARCC1 and miR-140-3p in the SW620 cell line. The effects of circSMARCC1 and miR-140-3p on cell proliferation were investigated using CCK8 and colony formation assays, respectively. The effects of circSMARCC1 and miR-140-3p on cell migration and invasion were determined using Transwell assay. The binding relationship between circSMARCC1 and miR-140-3p was further assessed by bioinformatics, ChIRP analysis and double luciferase reporter assay.

Results: The expression of circSMARCC1 in the CRC tissues and four cell lines is significantly increased, and circSMARCC1 and miR-140-3p are negatively correlated with expression level in the tissue. The downregulation of circSMARCC1 decreased CRC cell viability and suppressed metastasis in vitro and inhibition of protein (MMP-2, MMP-9, VEGF) expression. miR-140-3p is downregulated in CRC tissues; miR-140-3p mimics inhibited SW620 cell viability, migration and invasion, and miR-140-3p inhibitors reversed the effect of circSMARCC1 downregulation on cell proliferation, migration and invasion in CRC cells.

Conclusion: circSMARCC1 competitively combined with miR-140-3p and functioned through a circSMARCC1/miR-140-3p/MMPs axis as a CRC carcinogen, demonstrating its potential as a biomarker for CRC treatment.

Keywords: circSMARCC1, colorectal cancer, miR-140-3p, cell proliferation, MMP pathway

Introduction

Colorectal cancer (CRC) is one of the most common types of cancer affecting humans, and its incidence rate is increasing annually.^{1,2} The occurrence of CRC is usually related to personal habits, age, and lifestyle. Generally, an imbalance in the intestinal microflora and a variety of regulatory factors can induce colon cancer.³⁻⁵ As to CRC, gene mutations induce its occurrence and progression.^{6,7} The pathogenesis of CRC involves a complex and multistep molecular pathway, but its exact mechanism still needs to be elaborated. Therefore, a novel biomarker of CRC progression may provide an important insight into CRC therapy.

Circular RNAs (circRNAs) are widely distributed in mammalian cells and usually consist of hundreds of nucleotides.^{8,9} They can interact with microRNAs (miRNAs) and function as transcriptional or post-transcriptional factors for gene expression regulation.^{10,11} In contrast to linear RNAs, circRNAs can form stable and continuous

Correspondence: Xiao-ming Qiu
Tel +86-5972205108
Email abcrtom@163.com

covalently closed rings and do not easily degrade.^{12,13} Most circRNAs have conserved sequences and exhibit specific expression patterns depending on tissue or developmental stage. As competing endogenous RNAs (ceRNAs), circRNAs can be used as the regulatory factors of microRNA sponges and in altering the activities of miRNAs, which are endogenous 22 nt-long RNAs.^{9,11} Subsequently, circRNAs directly target mRNA sites to modify gene expression factors.¹⁴ Evidence shows that circRNAs have specific functions in CRC development. circRNAs have great potential as regulatory factors for biological functions and tumor development and a biomarkers for tumor therapy. However, a large number of circRNAs remain unidentified.

In our study, we found that has_circ_0003602 (circSMARCC1) is highly expressed in CRC tissues and cells. The downregulation of circSMARCC1 suppresses CRC cell viability and metastasis and is associated with the inactivity of matrix metalloproteinases (MMPs). We showed that circSMARCC1 directly targets miR-140-3p. Furthermore, we found that the downregulation of circSMARCC1 can increase miR-140-3p level. These results showed that circSMARCC1 acts as a tumor promoter that regulates miR-140-3p. Therefore, circSMARCC1 is a promising biomarker for CRC.

Materials and Methods

Clinical Samples

A total of 80 fresh clinical CRC tissue samples and adjacent tissues were obtained from Longyan First Hospital Affiliated to Fujian Medical University. The study was authorized by the Ethical Committee of Longyan First Hospital Affiliated to Fujian Medical University. And all patients provided written informed consent, and that this was conducted in accordance with the Declaration of Helsinki.

Cell Culture and Transfection

NCM460, SW620, HCT116, HT29, and SW480 cell lines were purchased from Bena Culture Collection. The cells were cultivated in fresh dulbecco's modified eagle medium (DMEM) (Gibco, NY, USA) containing 10% FBS at 37 °C and in 5% CO₂. The SW620 cell line was used for subsequent treatment. Small interfering RNAs targeting circSMARCC1 (si-circSMARCC1#1/2/3; see [Supplementary Table](#) for its primer sequence), miR-140-3p mimics, and an miR-140-3p inhibitor were obtained from GenePharma Company (Shanghai,

China). For cell transfection, SW620 cells were transiently transfected with Lipofectamine 2000 (Invitrogen) according to the manufacturer's protocol to a final concentration of 50 nM for miR-140-3p mimics/NC or inhibitors/NC and 50 nM for circSMARCC1. After 24 or 48 h of transfection, the cells were harvested for subsequent experiments. All the experiments were carried out independently three times.

RNA Isolation and qRT-PCR Analysis

TRIzol (Invitrogen, Carlsbad, USA) was used in isolating RNA from the SW620 cells or tissue samples according to the manufacturer's procedure, and genomic DNA was removed. miRNA was extracted and purified using an mirVana™ miRNA isolation kit (Invitrogen, Carlsbad, USA). RNase R was added to purify total RNA, which was then reverse-transcribed into cDNA. qPCR was conducted, and GoTaq® qPCR master mix (Promega, USA) was used. All the primer sequences were synthesized using Sangon Biotech (Shanghai, China; [Supplementary Table](#)). miRNA was used as a stem-loop primer, and GAPDH was used as the reference gene for circRNA and mRNA. U6 was used as an internal control for miRNA. The amplification processes of the reaction were as follows: preparation at 95 °C for 5 min, denaturation at 95 °C for 10 s, annealing at 60 °C for 30 s, and extension at 72 °C for 30 s, and the reaction was performed for 40 cycles. All the experiments were run in triplicate for each sample. The expression levels of the target genes were calculated using the comparative delta-delta CT method ($2^{-\Delta\Delta CT}$).

Stability Analysis of CircSMARCC1

For actinomycin D treatment, 2 µg/mL actinomycin D was injected to the SW620 cells. RNA was then extracted after 0, 4, 8, 12, and 24 h of treatment. For RNase R treatment, the total RNA of the SW620 cells was extracted and then treated with three units of RNase R for 30 min at 37 °C. The expression levels of circSMARCC1 and its linear subtype were detected. The primer sequences are provided in [Supplementary Table](#).

Fluorescence in situ Hybridization

Transfected cells were washed with CSK buffer solution after incubation at 4 °C for 10–12 min and then air-dried. A hybrid buffer solution with a probe (DIG-labelled circSMARCC1 probe or Cy3-labelled miR-140-3p probe) was denatured at 76 °C for 10 min, and

5 μ L of hybrid mixture was dropped on each climbing plate, which was then covered with a cover glass and sealed with rubber. The climbing slides were placed in a wet dark box at 37 °C for overnight hybridization. The cover glass of each slide was removed after hybridization. The climbing slides were washed with 50% formamide at 42 °C for 5 min. Remove the cover slides and wash them twice in PBS. Excess liquid was removed, and antifade Regent seal was applied for observation under a fluorescence microscope.

CCK8 Assay

The viability of the SW620 cells was detected using WST8 (Roche Biochemicals, Mannheim, Germany). SW620 cells were cultured in a 96-well plate with a density of 1×10^5 cells/well and incubated at 37 °C for 24, 48, and 72 h. CCK8 (10 μ L) was injected to each well for 1 h, then cell viability was detected under an absorbance wavelength of 450 nm. All the experiments were carried out independently three times.

Colony Formation Assay

SW620 cells were cultured in a six-well plate (100 cells/well in each well) and stained with 1 mL of 0.1% crystal violet (Sigma-Aldrich, MO, USA). Colony size ($\geq 50 \mu\text{m}$) was and the number of colonies were determined. The results of three independent assays were averaged.

Transwell Assay

Migration and invasion were measured using a polycarbonate membrane Boyden chamber. Transfected SW620 cells were first treated with trypsin, resuspended in DMEM, and added to an 8 μm -pore polycarbonate membrane Boyden chamber with or without 25 mg of Matrigel (BD Biosciences, CA, USA). DMEM with 10% FBS was added to the lower chamber. After 24 h of incubation, the cells migrated to the bottom surface. The migration and invasion cells were acquired from counting three fields per membrane.

Antisense Oligomer Pulldown ChIRP Analysis

ChIRP analysis was performed according to the published protocols.¹⁵ circSMARCC1 anti-sense DNA probes with BiotinTEG at 3-prime end were designed using online probe designer (singlemoleculefish.com) and produced by Sangon Biotech (Shanghai, China)

1. AAGTATCAAGCTTCTCTGGC-Bio; 2. TCTTGACATGAGCTTCAACC-Bio; 3. TTTCTGACTGACTGAAGGG-Bio; 4. GAGTACGACTTCC AACATGT-Bio). Cells were collected and subjected to crosslink with 3% formaldehyde. The crosslinked cells were lysed and sheared into 100–500 bp DNA fragments by sonicating in a 4 °C water bath at highest setting with 30 s ON, 45 s OFF pulse intervals. circSMARCC1 biotinylated probes were separated into odd and even two pools to hybridize with RNA at 37 °C for 4 h with shaking. LacZ probes were used as a negative control. qRT-PCR was performed with RNA samples to confirm circSMARCC1 retrieval. Interaction of circSMARCC1 with miR-140-3p examined by qPCR analysis. Probes used in this study are listed in [Supplementary Table](#).

Dual-Luciferase Activity Assay

The 3'UTR of circSMARCC1 (circSMARCC1-WT) and its mutant (circSMARCC1-Mut) were synthesized and inserted to a psiCHECKTM-2 vector (Promega, Madison, USA). After the SW620 cells reached a density of ~80%, they were transfected with reporter plasmid circSMARCC1-WT/circSMARCC1-Mut and miR-140-3p mimics/miR-140-3p inhibitor. Lipofectamine 2000 was used. As an internal control, all the cells were transfected with psiCHECKTM-2 plasmid. After transfection, relative luciferase activity was finally detected. All the experiments were performed independently three times.

Western Blot Analysis

The extracted proteins at equal volumes were injected to a sodium dodecyl sulfate–polyacrylamide gel and then transferred to a nitrocellulose filter membrane (Millipore, USA). The treated membrane was washed with TBST buffer, blocked with BSA, and incubated with antibodies. After 1 day, the proteins were incubated with a secondary antibody. Finally, the proteins were visualized using ECL-plus reagents and analyzed with Image J. The antibodies used in the study were anti-MMP2 (Abcam, Cambridge, MA), anti-MMP9 (Abcam, Cambridge, MA), and anti-VAGE (Ivitroge, USA). All the experiments were performed independently three times.

Statistical Analysis

All the data were expressed as means and standard deviations (SD). The statistical analysis was performed using

Graphpad Prism 6.0 (San Diego, USA). Student's *t*-test (two tailed) was performed. A *p* value of <0.05 was considered statistically significant.

Results

CircSMARCC1 Was Highly Expressed in CRC Tissues and Cell Lines

We used qRT-PCR to detect the expression level of circSMARCC1 in CRC tissues ($n = 40$) and cell lines. circSMARCC1 increased 1.87 fold on average compared with that in the adjacent tissues ($n = 40$; $p < 0.05$; [Figure 1A](#)). Similar results were obtained from the CRC cell lines (SW620, HCT116, HT29, and SW480) compared with normal colon mucosal epithelial cell (NM460; $p < 0.05$; [Figure 1B](#)). circSMARCC1 showed the highest expression in SW620. Thus we used SW620 cells in subsequent experiments.

We investigated circSMARCC1 in the occurrence and progression of colon cancer. We detected the stability and localization of circSMARCC1. After treatment with actinomycin D, the expression level of circSMARCC1 remained unchanged, and the expression of the linear mRNA gene decreased, indicating that circSMARCC1 was stable ($p < 0.05$; [Figure 1C](#)). After RNase R treatment, the expression level of circSMARCC1 remained unchanged, and the expression level of linear mRNA decreased, indicating that circSMARCC1 was stable ($p < 0.05$; [Figure 1D](#)). These results indicated that circSMARCC1 has a stable characteristic. Fluorescence in situ hybridization assay showed that circSMARCC1 was located in the cytoplasm ($p < 0.05$; [Figure 1E](#)).

Downregulated CircSMARCC1 Inhibits CRC Cells Proliferation, Migration, and Invasion in vitro

To investigate the biological functions of circSMARCC1 in CRC, we designed three small interfering RNAs (siRNAs) targeting the junction sites of circSMARCC1 and used them to silence circSMARCC1 expression in SW620 cells. These siRNAs obviously decreased circSMARCC1 expression level. We selected si-circSMARCC1#2 for subsequent experiments because it had the highest inhibitory efficiency ($p < 0.05$; [Figure 2A](#)). The CCK8 experiment showed that circSMARCC1 knockdown significantly inhibited cell proliferation in the SW620 cells ($p < 0.05$; [Figure 2B](#)). Cell colony-forming ability was measured on the basis

of clonal formation ($p < 0.05$; [Figure 2C](#)), and down-regulated circSMARCC1 significantly suppressed cell proliferation in these cell lines. Moreover, Transwell invasion assay demonstrated that circSMARCC1 silencing markedly impeded SW620 cell migration ($p < 0.05$; [Figure 2D](#)) and invasion ($p < 0.05$; [Figure 2E](#)) by 71% and 68%, respectively. These data indicated that the silencing of circSMARCC1 can retard the progression of CRC cells. Furthermore, the expression of MMP-2 and MMP-9 was detected. As shown in [Figure 2F](#) and [G](#), downregulated circSMARCC1 resulted in low mRNA level and circSMARCC1 expression level, thereby significantly decreasing MMP-2, MMP-9, and VEGF levels. These results revealed that downregulated circSMARCC1 suppresses cell viability, migration, and invasion by directly downregulating MMP-related markers in CRC cells.

CircSMARCC1 Can Sponge MiR-140-3p in CRC Cell Lines

To determine whether circSMARCC1 can sponge miR-140-3p in CRC cell lines, a 3' terminal-biotinylated-circSMARCC1 probe was designed. The probe was used in determining which miRNAs potentially interact with the potent molecular mechanism of circSMARCC1 in CRC cells. We detected the expression level of miR-140-3p in CRC tissues. miR-140-3p was significantly downregulated in the CRC tissues ($p < 0.05$; [Figure 3A](#)) and showed a negative relationship with circSMARCC1 expression ([Figure 3B](#)). We further tested the influence of circSMARCC1 on the expression level of miR-140-3p. qRT-PCR results showed that downregulated circSMARCC1 significantly promoted miR-140-3p level ($p < 0.05$; [Figure 3C](#)). In addition, the fluorescence indicated that circSMARCC1 and miR-140-3p were co-located in the cytoplasm ($p < 0.05$; [Figure 3D](#)). Luciferase report assay showed that circSMARCC1 directly targeted ZmiR-140-3p by directly inhibiting its expression. The co-transfection of circSMARCC1 wild-type (WT) or mutation (MUT) with miR-140-3p mimics showed that miR-140-3p can effectively inhibit circSMARCC1 luciferase activity ($p < 0.05$; [Figure 3E](#)). ChIRP assay illustrated that compared with LacZ, miR-140-3p was obviously enriched in the pellet pulled down by circSMARCC1 ($P < 0.05$, [Figure 3F](#)). These results indicated that circSMARCC1 is a potent target of miR-140-3p.

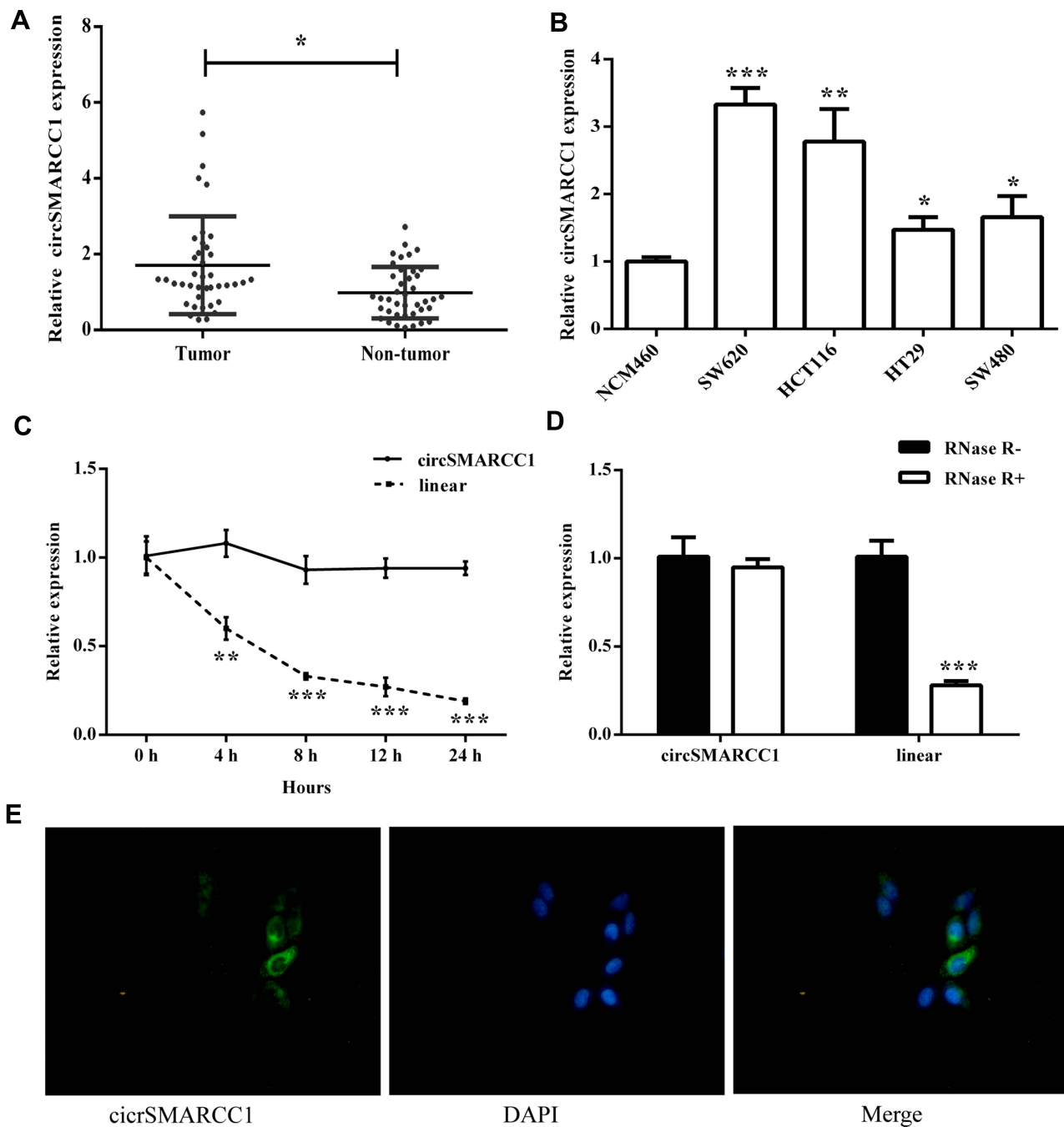


Figure 1 circSMARCC1 was upregulated in the CRC tissues and cell lines. (A) The expression level of circSMARCC1 in CRC tissues (n = 40) and adjacent tissues (n = 40) was detected by qRT-PCR. (B) The expression level of circSMARCC1 in the cultured cell lines was examined using qRT-PCR. (C) The mRNA expression of circSMARCC1 on CRC cells treated with actinomycin D. (D) The mRNA expression of circSMARCC1 on CRC cells treated with RNase R. (E) The localization of circSMARCC1 (left) and DAPI (middle) was showed, and the merged picture was provided (right). All the results were expressed as mean \pm SD (n=3) for three separate experiments. *p < 0.05, **p < 0.01, and ***p < 0.001.

MiR-140-3p Inhibited Cell Viability, Migration, and Invasion

We screened effective miR-140-3p mimics (p < 0.05; Figure 4A) and then tested their effects on viability. CCK8 assay showed that upregulated miR-140-3p can inhibit cell viability (p < 0.05;

Figure 4B), consistent with clonal colony formation. miR-140-3p significantly suppressed CRC cell clonal formation (p < 0.05; Figure 4C). In addition, we measured the migration and invasive ability of miR-140-3p. We found that miR-140-3p remarkably reduced migration and invasion (Figure 4D and E).

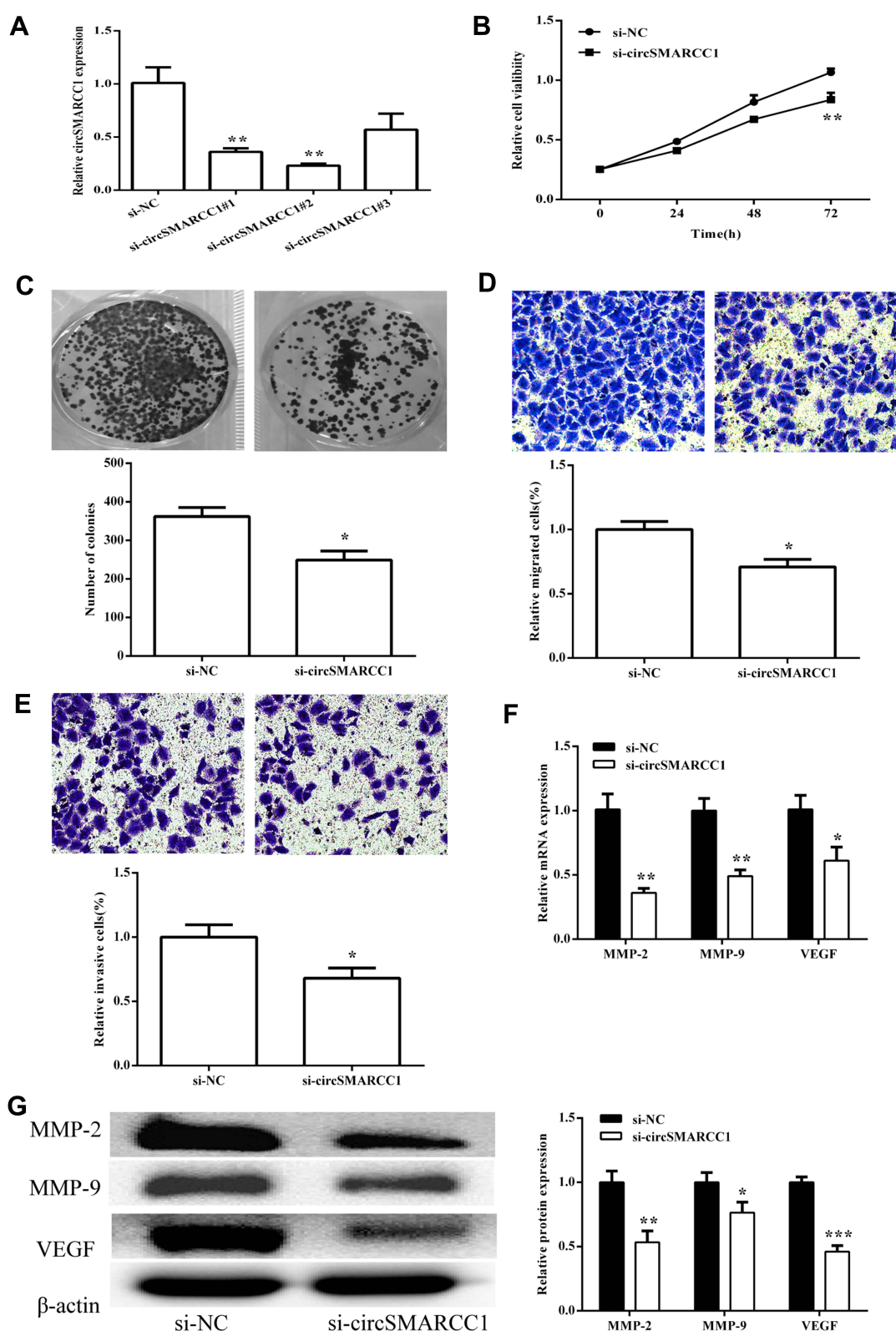


Figure 2 circSMARCC1 knockdown inhibited tumor growth in vivo. **(A)** Expression of circSMARCC1 was detected after transfection with three si-circSMARCC1. **(B)** Cell viability detected by CCK8 assay showed that the downregulation of circSMARCC1 decreased viability in the SV620 cells. **(C)** Colony formation was measured, and the results suggested that the downregulation of circSMARCC1 inhibited cell proliferation. The number of formed colonies was determined. **(D and E)** Transwell assay exhibited that the downregulation of circSMARCC1 suppressed SV620 cell migration and invasion. Migration and invasion cells were quantified. **(F)** The mRNA expression levels of MMPs were measured after transfection with si-circSMARCC1. **(G)** The protein expression level of MMPs was detected after transfection with si-circSMARCC1. Protein expression was quantified. All the results were expressed as mean \pm SD ($n = 3$) for three separate experiments. * $p < 0.05$, ** $p < 0.01$, and *** $p < 0.001$.

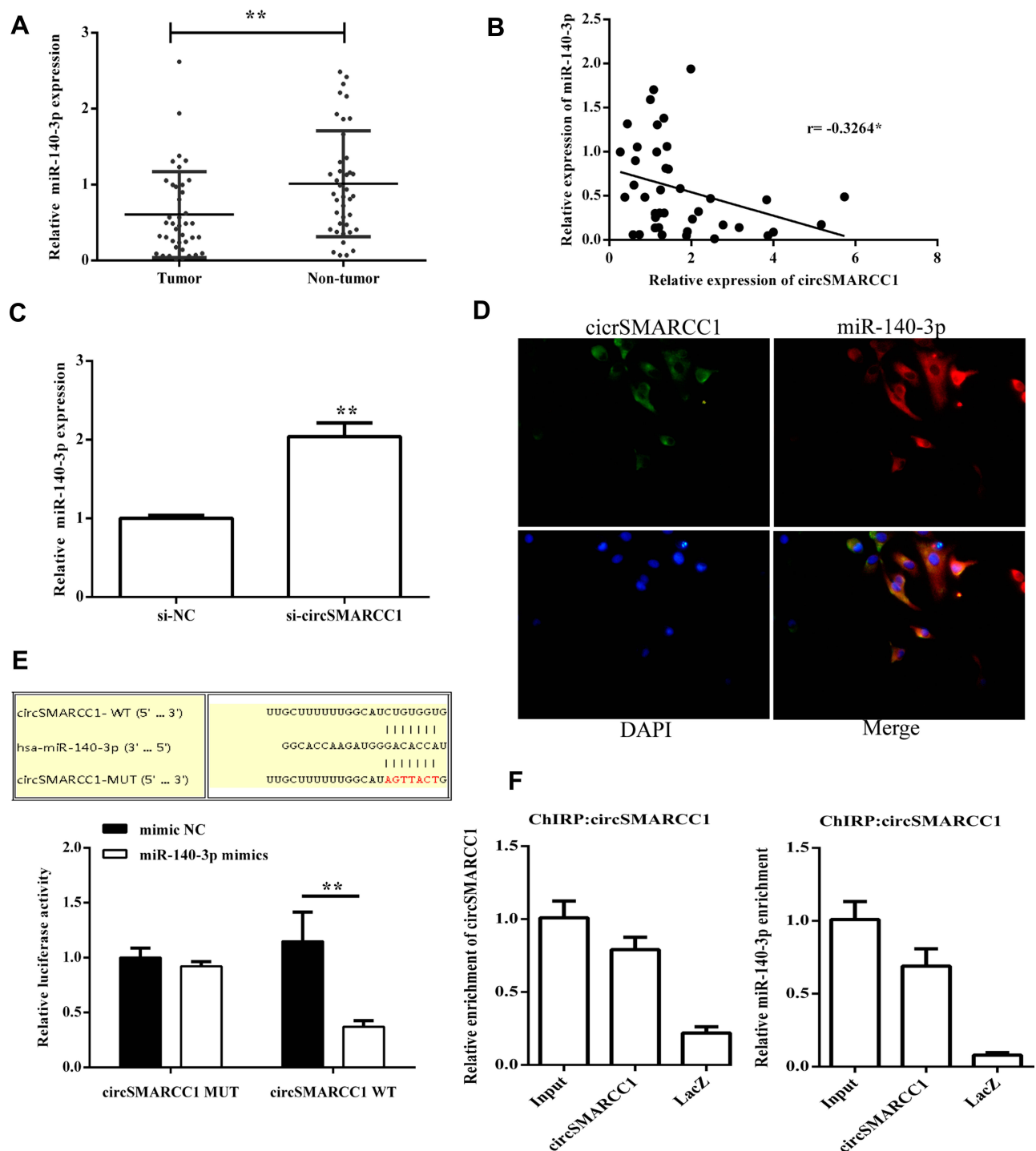


Figure 3 circSMARCC1 targeted miR-140-3p to regulate its expression. **(A)** The expression levels of miR-140-3p in CRC tissues ($n = 40$) and normal tissues ($n = 40$) were measured using qRT-PCR. **(B)** The correlation between circSMARCC1 expression and miR-140-3p expression in CRC tissues **(C)** Downregulation of circSMARCC1 promoted the mRNA expression of miR-140-3p. **(D)** The localization of circSMARCC1 and miR-140-3p. The cellular localization of circSMARCC1, miR-140-3p, and DAPI was detected, and the merged picture was provided. **(E)** Dual luciferase activity assay exhibited the binding affinity between circSMARCC1 and miR-140-3p. **(F)** The interaction between circSMARCC1 and miR-140-3p in SV620 cells was further verified through ChIRP assay. All the results were expressed as mean \pm SD ($n = 3$) for three separate experiments. $^*p < 0.05$, $^{**}p < 0.01$.

The influence of miR-140-3p on MMPs was assessed using qRT-PCR and Western blot analysis. We first tested the influence on circSMARCC1 expression. As shown in Figure 4F and G, miR-140-3p significantly inhibited

circSMARCC1 expression. Furthermore, miR-140-3p remarkably reduced the levels of MMP-2, MMP-9 and VEGF, which are closely associated with tumor aggressiveness.

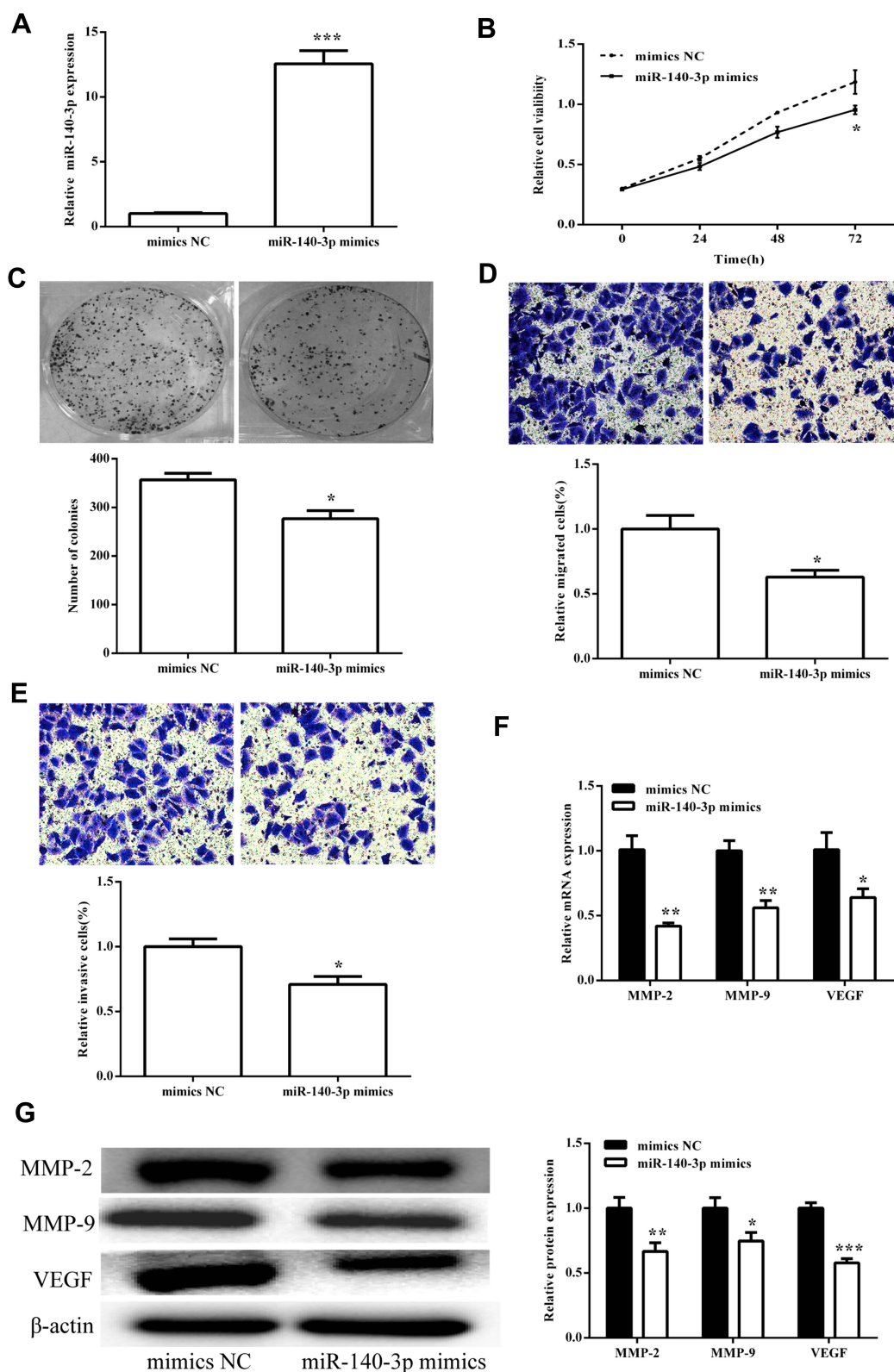


Figure 4 miR-140-3p inhibited cell viability and metastasis in the SW620 cells. (A) The expression of miR-140-3p was detected after transfection with miR-140-3p mimics. (B) Cell viability detected by CCK8 assay showed that miR-140-3p decreased viability in the SW620 cells. (C) Colony formation was measured, and the results suggested that miR-140-3p inhibited cell proliferation. The number of formed colonies was determined. (D and E) Transwell assay showed that miR-140-3p suppressed SW620 cell migration and invasion. Migration and invasion cells were quantified. (F) The mRNA expression levels of MMPs were measured after transfection with miR-140-3p mimics. (G) The protein expression levels of MMPs were detected after transfection with miR-140-3p mimics. Protein expression was quantified. All the results were expressed as mean \pm SD (n=3) for three separate experiments. * p < 0.05, ** p < 0.01, and *** p < 0.001.

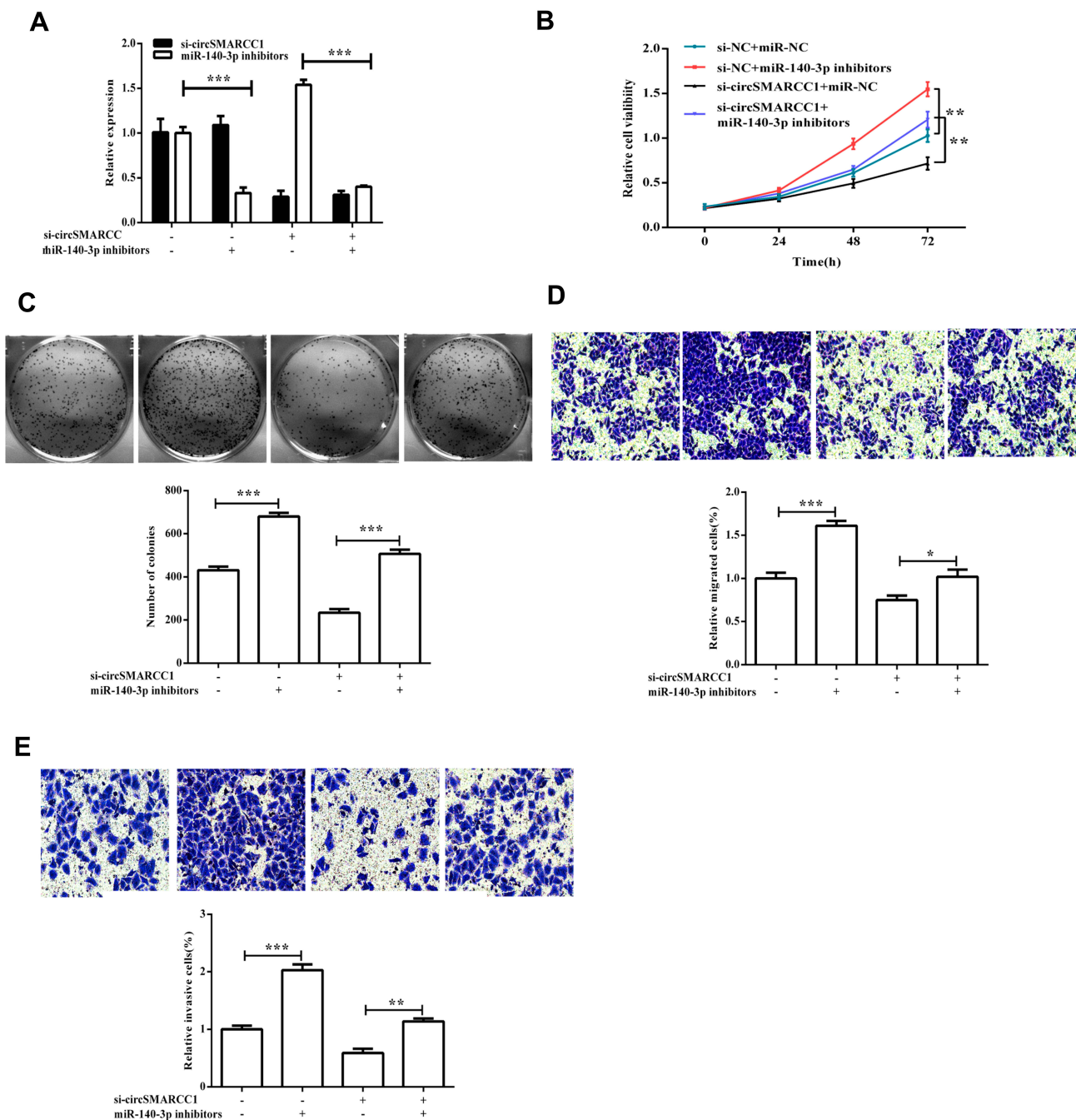


Figure 5 miR-140-3p inhibitors reversed the effect of circSMARCC1 downregulation on cell proliferation, migration, and invasion in the CRC cells. **(A)** The mRNA expression level of circSMARCC1 and miR-140-3p after transfection with si-circSMARCC1 and miR-140-3p inhibitors. **(B and C)** Cell viability and colony formation were measured after transfection with si-circSMARCC1 and miR-140-3p inhibitors. **(D and E)** Cell migration and invasion were measured. All the results were expressed as mean \pm SD ($n = 3$) for three separate experiments. * $p < 0.05$, ** $p < 0.01$, and *** $p < 0.001$.

MiR-140-3p Inhibitors Reversed the Effect of CircSMARCC1 Downregulation on Cell Proliferation, Migration, and Invasion in CRC Cells

To determine whether circSMARCC1 functioned through binding miR-140-3p, we determined whether miR-140-3p

inhibitors affect circSMARCC1 expression. The results exhibited that downregulated circSMARCC1 and miR-140-3p had no influence on circSMARCC1 expression but had a significant difference on miR-140-3p expression ($p < 0.05$; Figure 5A). Downregulated circSMARCC1 and miR-140-3p reversed viability and metastasis inhibition by

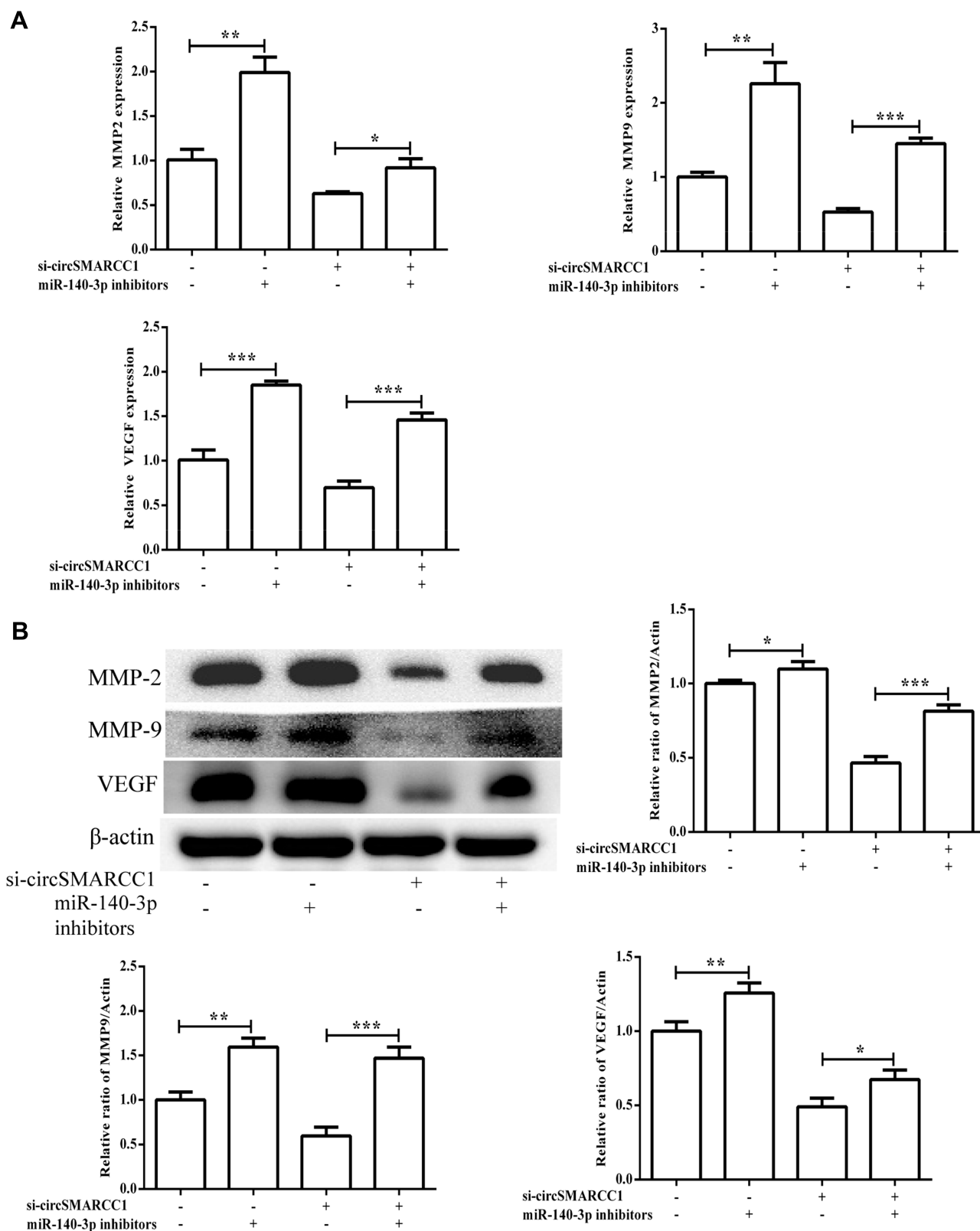


Figure 6 The expression of MMPs in the SW620 cells. **(A)** The mRNA expression levels of MMPs after transfection with si-circSMARCC1 and miR-140-3p inhibitors. **(B)** The protein expression levels of MMPs after transfection with si-circSMARCC1 and miR-140-3p inhibitors. All the results were expressed as mean \pm SD ($n = 3$) for three separate experiments. * $p < 0.05$, ** $p < 0.01$, and *** $p < 0.001$.

si-circSMARCC1 ($p < 0.05$; Figure 5B–E). These results indicated that circSMARCC1 and miR-140-3p have functions in CRC cells. Downregulated circSMARCC1 promoted miR-140-3p expression, but an miR-140-3p inhibitor has no influence on circSMARCC1 expression. As shown in Figure 6A and B, the miR-140-3p inhibitor significantly promoted the level of SMARCC1, downregulated circSMARCC1, and reversed the inhibitory effect of circSMARCC1. Additionally, the downregulation of circSMARCC1 and miR-140-3p resulted in a significant increase in MMP-2, MMP-9, and VAGE levels.

Discussion

Many studies showed that circRNA is closely related to CRC progression. The circRNA/miRNA/mRNA axis plays a critical role in CRC carcinogenesis, providing novel insights into the pathogenesis of CRC. In this study, we found that circSMARCC1 level was high in the clinical CRC tissues and four cell lines (SW620, HCT116, HT29, and SW480). Downregulated circSMARCC1 suppressed cell viability and metastasis by directly promoting miR-140-3p expression and inactivated the inhibition of MMP activity. MMPs large Ca^{2+} -dependent Zn^{2+} -containing endopeptidases. These enzymes can enhance cancer cell metastasis through degraded extracellular matrix (ECM) proteins.¹⁵ Among the more than 20 members of MMPs, gelatinases (MMP2 and MMP9) have important roles in the cleavage of ECM and serve as critical markers of tumor migration and invasion.^{16,17} circSMARCC1 exerts a critical effect on CRC cell progression. The downregulation of circSMARCC1 or upregulation of miR-140-3p is a potent method for CRC treatment. circSMARCC1 is a potential tumor promoter because it increases cell viability, migration, and invasion by enhancing MMPs and targeting the circSMARCC1/miR-140-3p/MMPs axis in CRC.

Recent studies showed circRNA is rich in microRNA (miRNA) binding sites, acting as an miRNA sponge in cells and thereby removing the inhibition of miRNA on its target genes and increasing the expression level of target genes. This mechanism of action is known as the competitive endogenous RNA (ceRNA) mechanism, which interacts with miRNAs associated with diseases. Additionally, circRNA plays an important regulatory role in diseases. Previous studies reported that circRNA expression levels in the cancer sera of patients with CRC significantly increased compared with the expression levels in healthy subjects.¹⁸ In addition, the expression of has-circ-001988

in CRC tissues decreased significantly, suggesting that has-circ-001988 is a biomarker.¹⁹ circRNAs can interact with miRNAs, then regulate gene expression in various cell processes. The influence of circRNAs on the occurrence and progression of CRC have received increasing attention in human tumor research in recent years. Therefore, circRNA is a promising biomarker and therapeutic target for CRC progression.

miR-140-3p can bind to binding sites on RNA sequences and induce the silencing of functional RNAs. In turn, circSMARCC1 molecules with the same miR-140-3p binding sites can compete for binding to miR-140-3p. Thus, two RNA molecules can exert regulatory effects through the bridge of miR-140-3p. Our study showed that the potential mechanistic activity for circSMARCC1 is associated with CRC progression. However, its other downstream targets (RNAs) and functions require comprehensive analysis.

Conclusion

circSMARCC1 is a tumor promoter in CRC. The downregulation of circSMARCC1 or upregulation of miR-140-3p suppressed the viability and metastasis in the SW620 cells. We further showed that the inhibitory effect acquired from the downregulated circSMARCC1 was mainly due to the upregulation of miR-140-3p expression and suppression of the MMP activity. Therefore, downregulated circSMARCC1 is a potent therapeutic target in CRC treatment.

Abbreviations

circRNA, circular RNA; CRC, colorectal cancer; miRNA, microRNA; ceRNAs, competing endogenous RNAs; MMPs, matrix metalloproteinases; ECM, extracellular matrix; SDS-PAGE, dodecyl sulfate, sodium salt (SDS)-Polyacrylamide gel electrophoresis.

Acknowledgments

We would like to acknowledge the helpful comments on this paper received from our reviewers. This work was supported by the Science and Technology Program of Longyan, China (No. 2019LYF12005).

Author Contributions

All authors made substantial contributions to conception and design, acquisition of data, or analysis and interpretation of data; took part in drafting the article or revising it critically for important intellectual content; gave final

approval of the version to be published; and agree to be accountable for all aspects of the work.

Disclosure

The authors report no conflicts of interest in this work.

References

1. Mughini-Gras L, Schaapveld M, Kramers J, et al. Increased colon cancer risk after severe salmonella infection. *PLoS One*. 2018;13(1):e0189721. doi:10.1371/journal.pone.0189721
2. Bray F, Ferlay J, Soerjomataram I, et al. Global cancer statistics 2018: GLOBOCAN estimates of incidence and mortality worldwide for 36 cancers in 185 countries. *CA Cancer J Clin*. 2018;68(6):394–424. doi:10.3322/caac.21492
3. Deoula MMSO, Huybrechts I, El Kinany K, et al. Behavioral, nutritional, and genetic risk factors of colorectal cancers in morocco: protocol for a multicenter case-control study. *JMIR Res Protoc*. 2020;9(1):e13998. doi:10.2196/13998
4. Bendinelli B, Palli D, Assedi M, et al. Alcohol, smoking and rectal cancer risk in a mediterranean cohort of adults: the European Prospective Investigation into Cancer and Nutrition (EPIC)-Italy cohort. *Eur J Gastroenterol Hepatol*. 2020;32(4):475–483.
5. Royston KJ, Adedokun B, Olopade OI. Race, the microbiome and colorectal cancer. *World J Gastrointest Oncol*. 2019;11(10):773–787. doi:10.4251/wjgo.v11.i10.773
6. Obuch JC, Ahnen DJ. Colorectal cancer: genetics is changing everything. *Gastroenterol Clin North Am*. 2016;45(3):459–476. doi:10.1016/j.gtc.2016.04.005
7. Muller MF, Ibrahim AEK, Arends MJ. Molecular pathological classification of colorectal cancer. *Virchows Arch*. 2016;469(2):125–134. doi:10.1007/s00428-016-1956-3
8. Li P, Chen S, Chen H, et al. Using circular RNA as a novel type of biomarker in the screening of gastric cancer. *Clin Chim Acta*. 2015;444:132–136. doi:10.1016/j.cca.2015.02.018
9. Memczak S, Jens M, Elefsinioti A, et al. Circular RNAs are a large class of animal RNAs with regulatory potency. *Nature*. 2013;495(7441):333–338. doi:10.1038/nature11928
10. Nair AA, Niu N, Tang X, et al. Circular RNAs and their associations with breast cancer subtypes. *Oncotarget*. 2016;7(49):80967–80979. doi:10.18632/oncotarget.13134
11. Hansen TB, Jensen TI, Clausen BH, et al. Natural RNA circles function as efficient microRNA sponges. *Nature*. 2013;495(7441):384–388. doi:10.1038/nature11993
12. Hentze MW, Preiss T. Circular RNAs: splicing's enigma variations. *EMBO J*. 2013;32(7):923–925. doi:10.1038/emboj.2013.53
13. Jeck WR, Sorrentino JA, Wang K, et al. Circular RNAs are abundant, conserved, and associated with ALU repeats. *RNA*. 2013;19(2):141–157. doi:10.1261/rna.035667.112
14. Bartel DP. MicroRNAs: genomics, biogenesis, mechanism, and function. *Cell*. 2004;116(2):281–297. doi:10.1016/S0092-8674(04)00045-5
15. Chu C, Zhang Q, da Rocha S, et al. Systematic discovery of Xist RNA binding proteins. *Cell*. 2015;161(2):404–416. doi:10.1016/j.cell.2015.03.025
16. Verma RP, Hansch C. Matrix metalloproteinases (MMPs): chemical-biological functions and (Q)SARs. *Bioorg Med Chem*. 2007;15(6):2223–2268. doi:10.1016/j.bmc.2007.01.011
17. Clark IM, Swingle T, Sampieri C, et al. The regulation of matrix metalloproteinases and their inhibitors. *Int J Biochem Cell Biol*. 2008;40(6–7):1362–1378. doi:10.1016/j.biocel.2007.12.006
18. Li Y, Zheng Q, Bao C, et al. Circular RNA is enriched and stable in exosomes: a promising biomarker for cancer diagnosis. *Cell Res*. 2015;25(8):981–984. doi:10.1038/cr.2015.82
19. Wang X, Zhang Y, Huang L, et al. Decreased expression of hsa_circ_001988 in colorectal cancer and its clinical significances. *Int J Clin Exp Pathol*. 2015;8(12):16020–16025.

Cancer Management and Research

Dovepress

Publish your work in this journal

Cancer Management and Research is an international, peer-reviewed open access journal focusing on cancer research and the optimal use of preventative and integrated treatment interventions to achieve improved outcomes, enhanced survival and quality of life for the cancer patient.

The manuscript management system is completely online and includes a very quick and fair peer-review system, which is all easy to use. Visit <http://www.dovepress.com/testimonials.php> to read real quotes from published authors.

Submit your manuscript here: <https://www.dovepress.com/cancer-management-and-research-journal>